



Taibah University

Journal of Taibah University Medical Sciences

www.sciencedirect.com



Original Article

## Activity prediction, structure-based drug design, molecular docking, and pharmacokinetic studies of 1,4-dihydropyridines derivatives as $\alpha$ -amylase inhibitors



Khalifa S. Aminu, M.Sc.<sup>a,b,\*</sup>, Adamu Uzairu, PhD<sup>a</sup>, Stephen E. Abechi, PhD<sup>a</sup>, Gideon A. Shallangwa, PhD<sup>a</sup> and Abdullahi B. Umar, PhD<sup>a</sup>

<sup>a</sup> Department of Chemistry, Ahmadu Bello University, Zaria, Nigeria

<sup>b</sup> Department of Pure and Industrial Chemistry, Bayero University, Kano, Nigeria

Received 11 July 2023; revised 16 October 2023; accepted 13 December 2023; Available online 22 December 2023

### المخلص

**أهداف البحث:** يشكل مرض السكري عبئا اقتصاديا كبيرا على البلدان في جميع أنحاء العالم. إن التكاليف المرتبطة بإدارة مرض السكري، بما في ذلك خدمات الرعاية الصحية والأدوية ومعدات المراقبة وخسائر الإنتاجية، كبيرة. ويقتد الاتحاد الدولي للسكري أن نفقات الرعاية الصحية العالمية المتعلقة بمرض السكري ومضاعفاته تتجاوز مئات المليارات من الدولارات سنويا. ولذلك، هناك حاجة ماسة لتطوير أدوية فعالة للغاية، وبأسعار معقولة، ويمكن للمجتمع الوصول إليها بسهولة.

**طريقة البحث:** تستكشف الدراسة الحالية التعديلات الهيكلية لمشتقات 1,4-ديهيدروبيريدين لتحديد مثبطات محددة للألفا أميليز بهدف تطوير أدوية أكثر فعالية ويمكن الوصول إليها لمرض السكري، وتم تقييم القدرة التنبؤية والملمزة للمركبات المصممة. كما تم إجراء دراسات التشابه الدوائي والحركية الدوائية للمركبات المعدلة.

**النتائج:** أشارت نتائج الدراسة إلى أن المعادلة الأولى أظهرت أعلى مستوى من الدقة بسبب توافقها مع معايير التقييم الداخلية والخارجية. علاوة على ذلك، أظهر تصميم نظائرها الخمسة القوية باستخدام تصميم الدواء القائم على الهيكل تفاعلاً إيجابياً عند مقارنته بالقلب والأكاربوز. بالإضافة إلى ذلك، أشارت الدراسات الشاملة حول الخصائص الشبيهة بالأدوية والحركية الدوائية لمركبات التصميم إلى سلامتها عن طريق الفم وملائمتها الدوائية الإيجابية.

**الاستنتاجات:** تظهر نظائرها التصميمية وعدا بتطوير عوامل جديدة لخفض السكر في الدم، مع سماتها الإيجابية وأدائها في الدراسة مما يجعلها مرشحة محتملة لمزيد من البحث في تحسين علاجات الحالات المرتبطة بارتفاع نسبة السكر في الدم.

**الكلمات المفتاحية:** مرض السكري؛ ديهيدروبيريدين؛ ألفا أميليز؛ الالتحام الجزيئي؛ التشابه الدوائي؛ الحركية الدوائية

### Abstract

**Objectives:** Diabetes places a substantial economic burden on countries worldwide. The costs associated with diabetes management, including healthcare services, medications, monitoring equipment, and productivity losses, are substantial. The International Diabetes Federation has estimated that global healthcare expenditures associated with diabetes and its complications exceed hundreds of billions of dollars annually. Therefore, a critical need exists to develop drugs that are highly effective, affordable, and easily accessible to society.

**Methods:** This study explored the structural modification of 1,4-DHP derivatives to identify specific  $\alpha$ -amylase inhibitors, with the aim of developing more effective and accessible drugs for diabetes. We evaluated the activity and binding ability of the designed compounds. In addition, we performed drug-likeness and pharmacokinetic studies on the modified compounds.

**Results:** Equation (1) had the highest accuracy, on the basis of internal and external assessment parameters, including  $R^2_{int} = 0.852$ ,  $R^2_{adj} = 0.803$ ,  $Q^2_{cv} = 0.731$ , and  $R^2_{ext} = 0.884$ . Moreover, the five potent analogs identified through structure-based drug design demonstrated a

\* Corresponding address: Department of Chemistry, Ahmadu Bello University, Zaria, Nigeria.

E-mail: aminukhalifa1@yahoo.com (K.S. Aminu)

Peer review under responsibility of Taibah University.



Production and hosting by Elsevier

more favorable interaction than observed for the template or acarbose. Additionally, comprehensive studies on the drug-like properties and pharmacokinetics of the designed compounds supported their oral safety and favorable pharmacokinetic profiles.

**Conclusions:** The designed analogs show promise for developing new hypoglycemic agents. Their positive attributes and performance suggest that they may potentially serve as candidates for further research in improving treatments for high blood sugar-associated conditions.

**Keywords:**  $\alpha$ -Amylase; Diabetes; Dihydropyridines; Drug-likeness; Molecular docking; Pharmacokinetics

© 2023 The Authors. Published by Elsevier B.V. This is an open access article under the CC BY-NC-ND license (<http://creativecommons.org/licenses/by-nc-nd/4.0/>).

## Introduction

Despite strong intervention measures, type 2 diabetes mellitus (T2DM) remains prevalent worldwide. The use of hypoglycemic agents in combination with substantial lifestyle changes is central to disease management.<sup>1</sup> Because diabetes is an endocrine and metabolic disorder characterized by diminished insulin secretion and/or activity, patients with chronic conditions may experience serious health challenges including neuropathy, retinopathy, and cardiovascular complications.<sup>2</sup> Although many drugs are available for disease management, they have pronounced adverse effects; consequently, scientific communities must search for new drug candidates with low or absent adverse effects.<sup>3</sup>

For decades, the key strategies used to control diabetes focused on controlling dietary carbohydrate digestion. Starch is an important molecule serving as a primary source of energy for most (if not all) animal species.<sup>4</sup> The digestion of starch depends largely on four key  $\alpha$ -glucosidases: salivary and pancreatic  $\alpha$ -amylases, maltase-glucoamylase, and sucrase-isomaltase. The synergistic activities of these enzymes ultimately lead to the generation of glucose for absorption.<sup>5</sup> Therefore, studies focusing on these enzymes could greatly aid in controlling postprandial blood glucose levels and hence decrease the risk of complications in patients with T2DM.

Recently, amylases, membrane-bound enzymes, have gained considerable interest in the control of diabetes mellitus and other related metabolic diseases. The enzyme is produced by the salivary glands and aids in the initial digestion of starch molecules into breakdown products such as maltose.<sup>6</sup> Among amylase types,  $\alpha$ -,  $\beta$ -, and  $\gamma$ -amylases are crucial in the breakdown of carbohydrates. The  $\alpha$ -amylases catalyze the cleavage of  $\alpha$ -1,4 glycosidic linkages in amylose, thus yielding products such as dextrin and glucose units, and ultimately leading to hyperglycemia and the development of T2DM.<sup>7</sup> A recent review has described the promising effects of  $\alpha$ -amylase inhibitors on the treatment of T2DM.<sup>8</sup>

In our continued efforts to search for novel antidiabetic agents, we explored the potential of 1,4-dihydropyridine

(1,4-DHP) derivatives against human  $\alpha$ -amylases. Dihydropyridines are a class of heterocyclic nitrogen containing compounds with a wide spectrum of biological activities.<sup>9</sup> Specifically, the 1,4-DHP nucleus is an important scaffold found in many drugs. Yousuf et al.<sup>22</sup> have recently indicated the strong in vitro inhibitory activities of several 1,4-DHP derivatives against  $\alpha$ -amylase. Their findings have paved the way to further investigations of the scaffold to discover novel anti-diabetic agents.

In the present study, structural modification of 1,4-DHP derivatives was performed alongside molecular docking studies to identify specific inhibitors of  $\alpha$ -amylase. In addition, quantitative structure–activity relationship (QSAR) and pharmacokinetic analyses of the modified compounds were performed. The findings may provide insights for researchers working in this field.

## Materials and Methods

### *Creation of datasets, structure design, and optimization*

Twenty-six compounds derived from 1,4-DHPs were selected from the work of Yousuf et al.<sup>22</sup> These compounds were evaluated for their inhibitory concentrations ( $IC_{50}$ ) toward  $\alpha$ -amylase, and the obtained values were expressed in micromolar ( $\mu M$ ) concentrations. The  $IC_{50}$  values were standardized by conversion to  $pIC_{50}$  with Equation (1):<sup>2</sup>

$$pIC_{50} = -\log(IC_{50} \times 10^{-6}) \quad (1)$$

Next, the reported compounds were visually represented in 2D with ChemDraw version 12.0 software and automatically transformed into 3D structures with Spartan version 14 software.<sup>10</sup> The optimization of the compounds was performed on the basis of density functional theory with the Bee-3-Lee Yang Par method and 6-311G\* as the basis set. This approach was aimed at alleviating constraints and determining the most stable geometry for the reported compounds.<sup>11</sup> Finally, the optimized compounds were saved in a structure data file format (sdf).

### *Docking studies on the derivatives of 1,4-DHP*

Docking studies were conducted on all derivatives of 1,4-DHPs to investigate the interactions between the active pocket of  $\alpha$ -amylase and the derivatives. This analysis was aimed at gaining insight into the interaction patterns, to guide the design of highly active compounds with improved efficacy.<sup>12</sup>

### *Evaluation of descriptors, pretreatment of data, and division of datasets*

To obtain descriptors for each compound, we imported the optimized 3D structures of the reported compounds into the Pharmaceutical Data Exploration Laboratory descriptor tool kit, and performed calculations. Additionally, data pre-treatment software version 1.2 was used to pre-process the calculated descriptors, and manual pre-treatment was performed to remove undesirable descriptors.<sup>13</sup> The dataset was then divided into a training (internal) set and a test (external)

set with the Kennard–Stone algorithm method, as implemented in Data Division software.<sup>14</sup> The training set consisted of 21 compounds, whereas the test set comprised five compounds.

#### Construction of models, validation, and statistical evaluation of the selected model

The QSAR model was created in Material Studio version 8.0 software. First, a set of compounds, denoted the training set, was imported into the software.<sup>15</sup> The genetic function approximation (GFA) method was used for model generation. In GFA, the  $pIC_{50}$  values (a measure of the biological activity) were considered dependent variables, and the molecular descriptors (properties of the compounds) served as independent variables. Model performance was assessed with Friedman's lack of fit scoring.<sup>16</sup> Several parameters were specified for the GFA approach. The equation length, which determines the complexity of the equations used in the model, was set to 5, including both the initial and maximum equation length. The mutation probability, a measure of the likelihood of changes occurring in the equations during optimization, was set to 0.1. The population and maximum generation parameters, which control the size and duration of the optimization process, were both set to 1000. The top four equations with the highest correlation were selected.<sup>2</sup> GFA is known for its ability to select descriptors that are highly correlated with activity and produce better models than stepwise regression methods.

After generation of the models, we evaluated their performance with three metrics: the square correlation coefficient of the training set ( $R^2_{int}$ ), adjusted square correlation coefficient ( $R^2_{adj}$ ), and cross-validation coefficient ( $Q^2_{cv}$ ). These metrics were used to assess the models' goodness of fit to the training data and their reliability in predicting the activity of new compounds.<sup>11</sup>

To validate the QSAR model externally, we used a separate set of compounds called the test set. The correlation coefficient ( $R^2_{ext}$ ) of the test set was calculated with Equation (2), and the model with the highest correlation was chosen. In an external regression equation, a value of  $R^2$  closer to 1 indicates a better fit, meaning that the model can accurately predict the activity of compounds that it has not previously encountered.<sup>3</sup>

$$R^2_{ext} = 1 - \frac{\sum (Y_{exp} - Y_{pred})^2}{\sum (Y_{exp} - Y_{train})^2} \quad (2)$$

where  $R^2_{ext}$  is the external correlation coefficient,  $Y_{exp}$  is the experimental activity,  $Y_{pred}$  is the predicted activity, and  $Y_{train}$  is the average internal compound.

The chosen model was evaluated on the basis of two key factors: the mean effect ( $M_x$ ) and the variance inflation factor (VIF). The mean effect of each descriptor in the selected model was used to assess the effect and contributions of the descriptor with Equation (3). Additionally, the combined effects of these descriptors, along with their respective mean effect values, provided insights into their influence on the activities of the investigated compounds.<sup>12</sup>

$$M_{x_j} = \frac{P_j \sum_{j=1}^q E_{ij}}{\sum_j P_j \sum_i E_{ij}} \quad (3)$$

where  $M_{x_j}$  is the mean effect of descriptor  $j$  in a model,  $P_j$  is the coefficient of descriptor  $j$  in that model,  $E_{ij}$  is the value of the descriptor in the data matrix for each molecule in the model building set,  $q$  is the number of descriptors in the model, and  $r$  is the number of molecules in the model building set.

Moreover, the VIF provides a measure of the inter-correlation among the descriptors used in the construction of the model.<sup>10</sup> The VIF values were calculated with the following equation:

$$VIF = \frac{1}{1 - S^2} \quad (4)$$

where  $VIF$  is the variance inflation factor, and  $S^2$  is the correlation coefficient of the selected model.

#### Applicability studies

The selected model was evaluated with a Williams plot, a graphical representation of standardized residuals plotted against leverage values.<sup>17</sup> This plot was used to identify any unusual or outlier molecules within the specified datasets. To conduct this assessment, we calculated the leverage values with the following equations:

$$W_i = Y_i (X^T X)^{-K} x_i^T \quad (5)$$

$$W^* = 3(C + 1)/T \quad (6)$$

In equation (5),  $W_i$  represents the leverage of a data point,  $Y_i$  denotes the descriptor variables for that point,  $X$  represents the design matrix, and the superscript  $T$  denotes matrix transpose. The leverage values indicate the influence of individual data points on the model's predictions.

In equation (6),  $W^*$  represents the warning leverage,  $C$  represents the number of descriptors, and  $T$  represents the number of data points. The warning leverage is a threshold value used to identify potential influential observations.

#### Structural modification of 1,4-DHP for the design of new therapeutic drugs

Structure-based drug design is a method using three-dimensional arrangement of target proteins to create and improve novel medications.<sup>19</sup> The process involves identifying the target, determining the structure of the protein, analyzing its binding sites, conducting virtual screens to identify potential drug candidates, optimizing these candidates through chemical modifications, and evaluating their biological activity.<sup>19</sup> In this study, compounds were chosen as templates for drug design on the basis of high binding scores. This selection was made to identify compounds with strong ability to bind the target protein, while minimizing any negative effects or unwanted interactions. By using these compounds as a reference or starting point, our goal was to design and develop more potent and selective drugs for the management of diabetes.

### Drug similarity and pharmacokinetic properties of the designed compounds

The evaluation of the drug similarity and pharmacokinetic properties of designed compounds is critical to ensure their bioavailability and safety in humans.<sup>20</sup> This evaluation is typically performed through in silico analyses, which involve in silico predictions and assessments. To assess the properties of the designed compounds, we used an online certified free web tool, SWISSADME (<http://www.swissadme.ch/index.php>), specifically designed for predicting and evaluating the drug-likeness and pharmacokinetic properties of small compounds.<sup>18</sup> Several rules and criteria were applied to determine how well the designed compounds conformed to drug-likeness and pharmacokinetic guidelines. The compounds' adherence to the Lipinski rule, Veber rule, Egan rule, and Muegge rule was assessed. These rules evaluate factors such as molecular weight, lipophilicity, and the presence of specific functional groups. Additionally, a bioavailability score was calculated to further evaluate the drug-likeness of the compounds; this score indicates how likely a compound is to be absorbed and distributed within the body.

Furthermore, the compounds were tested for their absorption, permeability, substrate potential, and potential to inhibit cytochrome P450 (CYP) enzymes. These tests help determine the compounds' pharmacokinetic profiles, including their ability to be absorbed by the body, their transport across biological barriers, and their potential interactions with enzymes involved in drug metabolism.<sup>21</sup>

### List of abbreviations

QSAR: quantitative structure activity relationship; GFA: genetic function approximation.

### Results

The derivatives' experimental activities were expressed in logarithmic form. The discrepancies between the experimental and predicted activities, referred to as the residuals, are shown in Table 1. The predicted  $pIC_{50}$  values for the internal set compounds were generally close to the experimental  $pIC_{50}$  values, and the MolDock scores for the internal set compounds ranged from  $-128.3$  to  $-159.1$ . Additionally, the predicted  $pIC_{50}$  values for the external set compounds were close to the experimental  $pIC_{50}$  values, with MolDock scores ranging from  $-134.1$  to  $-158.2$  (Table 1).

The findings from the four equations in Table 2 revealed that the first equation yielded the highest internal assessment ( $R^2_{int}$ ) score, 0.852, whereas the fourth equation had the lowest score, 0.838. In terms of adjusted  $R^2$  ( $R^2_{adj}$ ), the first equation performed best, with a value of 0.803, whereas the fourth equation had the lowest adjusted  $R^2$  score, 0.784. The second equation achieved the highest cross-validated  $Q^2$  ( $Q^2_{cv}$ ) value, 0.745, whereas the third equation had the lowest  $Q^2_{cv}$  score, 0.723 (Table 2). The external assessment ( $R^2_{ext}$ ) indicated that the first equation outperformed the others, with an  $R^2_{ext}$  score of 0.884,

whereas the fourth equation had the lowest  $R^2_{ext}$  value, 0.814 (Table 2).

The  $R^2_{int}$  value of 0.852 provided insight into the proportion of the total variation in the biological activity that could be explained by the equation, by indicating the selected equation's goodness of fit to the internal datasets. A higher  $R^2_{int}$  score suggests greater goodness of fit. The  $R^2_{adj}$  value of 0.803 increased a more reliable estimate of the equation performance and helped prevent overfitting. A higher  $R^2_{adj}$  score indicates a better equation performance. The  $Q^2_{cv}$  value of 0.731 suggested that the equation demonstrated good predictive ability for new compounds. Cross-validated  $Q^2$  is used to evaluate the equation's ability to predict the activity of new compounds. A higher  $Q^2_{cv}$  score indicates stronger predictive ability. The  $R^2_{ext}$  value of 0.884 revealed substantial variation in the external set data and suggested excellent predictive performance of the equation on external data. Therefore, the equation successfully captured the variability in the external set compounds.

Overall, given the highest internal and external assessment scores, the first equation appeared to be the most favorable.

Figure 1 illustrates the correlation between the experimental and predicted activities of both the internal and external datasets. The  $R^2$  value of the plot was close to 1, thereby demonstrating the reliability of the chosen equation. This finding was further supported by the plot of residuals against the experimental activities of the internal and external datasets in Figure 2. The standardized residuals were scattered around 0, thus indicating that the equation was free from any systematic errors. Consequently, Equation (1) accurately predicted the activities of the compounds.

The equation indicated ATS4i, GATS4c, VR3\_Dzp, VR3\_Dzs, and piPC9 as important descriptors (Table 3). The VIF values of these descriptors ranged from 2.70 to 8.58, and the mean effect values ranged from  $-0.30$  to 1.45 (Table 3). Additionally, the P-values of the descriptors were all below 0.05. The results indicated that the selected equation was valid and reliable (Table 3).

The Y-permutation test in Table 4 was used to determine whether the equation's predictions might have been due to chance. The activity matrix was randomly shuffled. To accept the QSAR equation as robust and reliable, the  $R^2$  and  $Q^2$  values were required to be low for multiple trials, and the coefficient of determination for Y-permutation was required to exceed 0.5. The  $R^2$  and  $Q^2$  values were 0.176 and  $-0.323$ , respectively, and the  $cRp^2$  was 0.705 (Table 4).

Figure 3 displays the Williams plot, which is used to identify compounds that deviate from the expected behavior in a specific equation. The plot compares the standardized residuals (a measure of the difference between observed and predicted values) against the leverage values (a measure of the extent to which an individual compound influences the equation). In this study, a cut-off leverage value of 0.86 was chosen to define compounds significantly affecting the equation's performance. Compounds with leverage values above this threshold were considered influential, because they greatly affected the equation's predictions. According to the plot, compounds 23, 25, and 26 from the test set had leverage values above the cut-off, thus

Table 1: The structures, experimental  $pIC_{50}$ , predicted  $pIC_{50}$ , residuals, and scores of the derivatives.

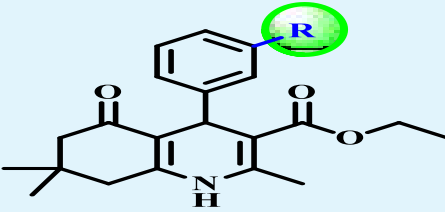
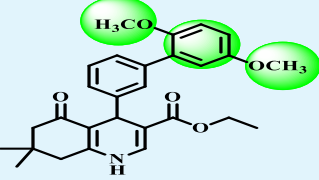
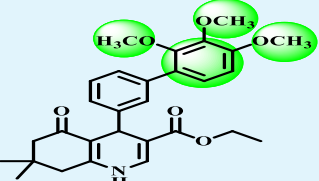
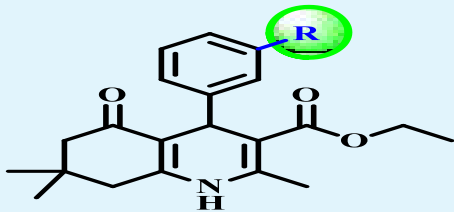
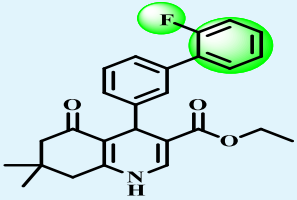
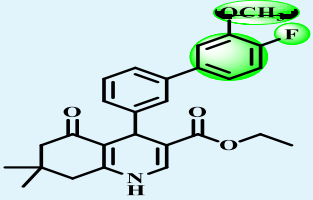
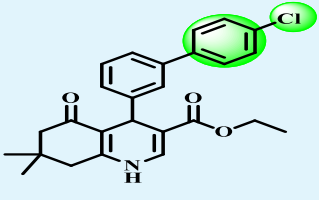
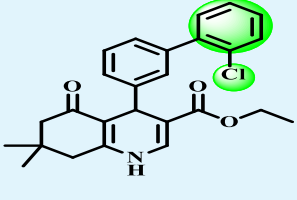
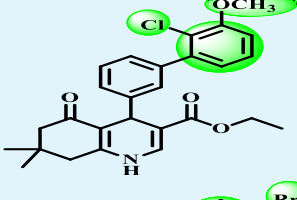
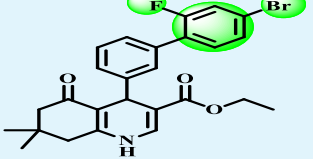
<i>R</i>	Experimental $pIC_{50}$	Predicted $pIC_{50}$	Residual	MolDock score	
Internal set compounds					
1		5.001	5.018	-0.016	-128.3
2		5.366	5.380	-0.014	-135.3
3		5.208	5.230	-0.022	-136.7
4		5.214	5.247	-0.033	-132.1
5		5.130	5.111	0.019	-144.2
6		5.186	5.161	0.026	-139.7

Table 1 (continued)

					
	<i>R</i>	Experimental $pIC_{50}$	Predicted $pIC_{50}$	Residual	MolDock score
7		5.161	5.190	-0.030	-130.4
8		5.292	5.295	-0.003	-139.2
9		5.333	5.214	0.118	-130.2
10		5.045	5.049	-0.004	-131.3
11		5.387	5.355	0.032	-137.6
12		5.228	5.292	-0.064	-123.4
13		5.309	5.273	0.036	-124.7

(continued on next page)

Table 1 (continued)

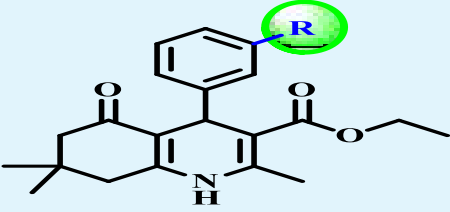
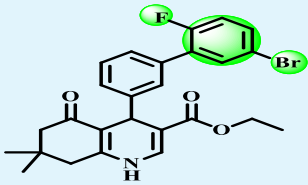
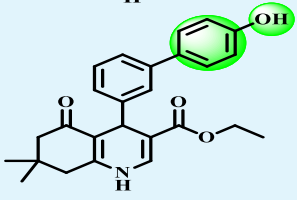
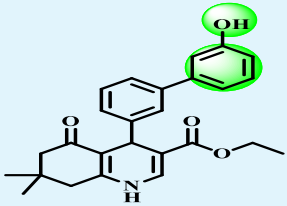
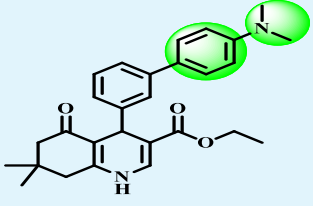
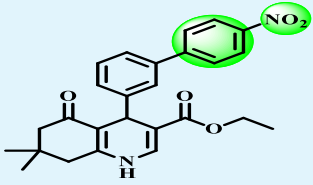
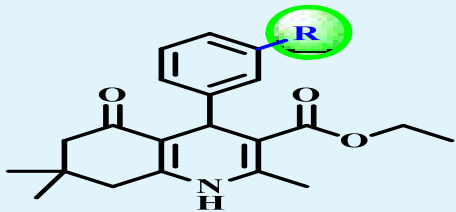
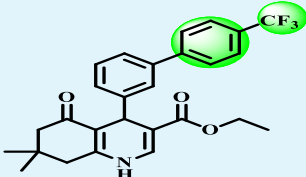
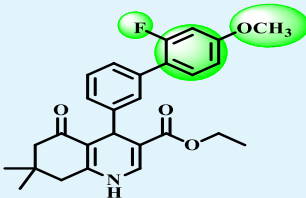
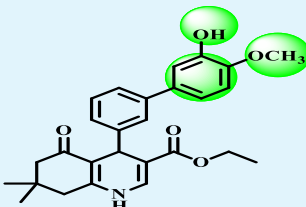
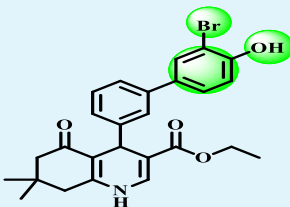
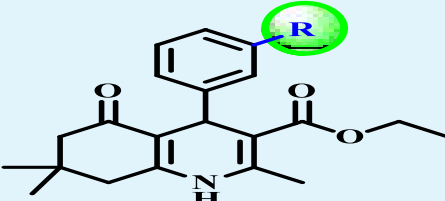
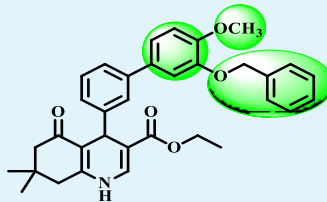
					
	R	Experimental $pIC_{50}$	Predicted $pIC_{50}$	Residual	MolDock score
14		5.136	5.171	-0.035	-135.0
15		5.200	5.245	-0.045	-131.6
16		5.283	5.255	0.029	-135.0
17		5.214	5.243	-0.029	-135.7
18		5.366	5.351	0.015	-147.0
19		5.221	5.220	0.001	-149.8
20		5.180	5.158	0.022	-137.3

Table 1 (continued)

					
	<i>R</i>	<i>Experimental pIC<sub>50</sub></i>	<i>Predicted pIC<sub>50</sub></i>	<i>Residual</i>	<i>MolDock score</i>
21		5.173	5.173	0.000	-136.7
<b>External set compounds</b>					
22		5.492	5.447	0.045	-142.1
23		5.400	5.307	0.093	-134.1
24		5.398	5.478	-0.080	-139.0
25		5.387	5.442	-0.054	-136.1

(continued on next page)

Table 1 (continued)

R	Experimental $pIC_{50}$	Predicted $pIC_{50}$	Residual	MolDock score
				
26	5.386	5.435	-0.049	-135.2
				
Acarbose	5.697	—	—	-136.1

indicating their potential influence on the equation. Additionally, compound 9 from the training set was identified as an outlier, because its standardized residual was outside the acceptable range of  $\pm 3$ .

#### Structure-based drug design and activity relationship studies

Structure-based drug design uses the three-dimensional structure of a target molecule to create a drug that binds the molecule. This method of drug design is based on the concept in which the structure of a molecule can be used to predict its function, and that by understanding the structure of a target molecule, a drug can be designed to interact with the target in a specific manner. In this study, compound 19 was used as a template for the design of new novel candidate (Figure 4).

The results of the study in Figure 5 showed that the addition of ( $-OCH_3$ ) and ( $-NO_2$ ) significantly enhanced the binding affinity of the compounds. For instance, the addition of nitro groups at the ortho positions increased

the score to  $-154.05$ . When a methoxy group was added at the ortho and meta positions, the score increased to  $-154.33$ , a value higher than those for the template and acarbose. This finding was probably due to stabilization through the resonance effect, which induced greater interaction between the designed compounds and the enzyme active site. Moreover, the calculated predicted activities of the designed compounds were higher than those of the template, thus demonstrating the potential for with electron-withdrawing and electron-donating groups to improve the antidiabetic activities of the compounds.

#### Molecular docking studies of the designed compounds

Molecular docking studies were conducted to gain insight into the nature of binding interactions and the amino acid residues contributing to the biological activity of the compounds. In this study, docking was performed on the five most active designed compounds at the binding pocket of the enzyme (PDB ID: 3TOP). The results are summarized in Table 5.

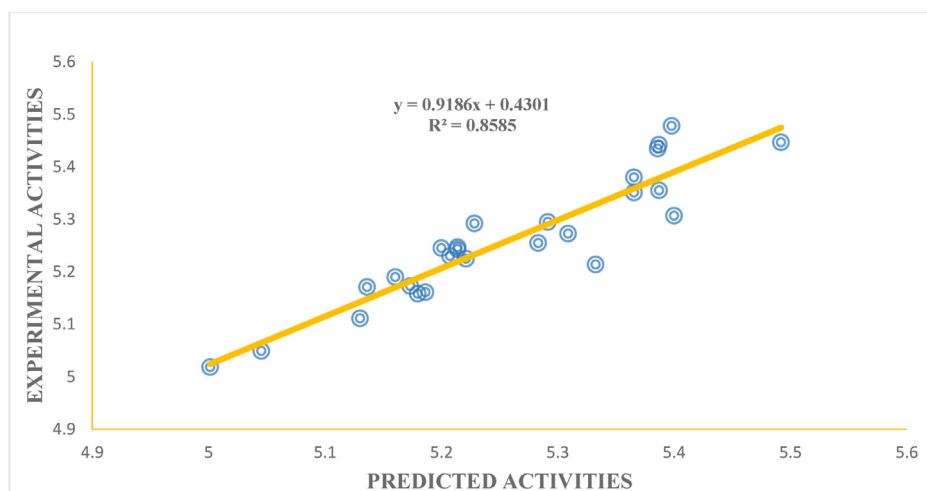
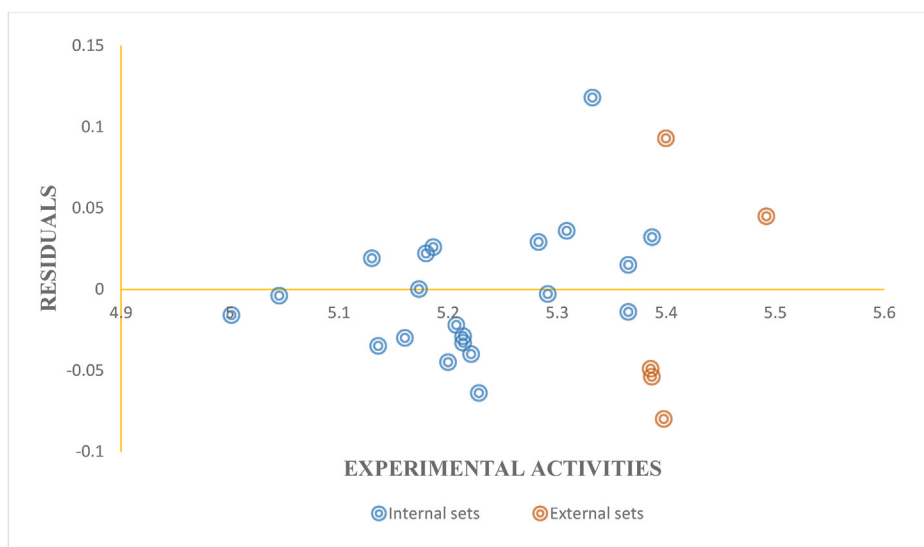


Figure 1: Plot of experimental and predicted activities for the internal and external datasets.

**Table 2: Internal and external assessment of the four equations generated.**

Equation	Internal Assessment	External Assessment
1 $Y = 4.131 \times 10^{-5} \cdot \text{ATS4i} - 2.123 \cdot \text{GATS4c}$ $+ 0.0736 \cdot \text{VR3\_Dzp} + 0.062 \cdot \text{VR3\_Dzs}$ $- 0.823 \cdot \text{piPC9} + 9.075$	$R^2_{\text{int}} = 0.852$ $R^2_{\text{adj}} = 0.803$ $Q^2_{\text{cv}} = 0.731$	$R^2_{\text{ext}} = 0.884$
2 $Y = 4.882 \times 10^{-5} \cdot \text{ATS3i} - 2.181 \cdot \text{GATS4c}$ $+ 0.069 \cdot \text{VR3\_Dzp} + 0.065 \cdot \text{VR3\_Dzs}$ $- 0.739 \cdot \text{piPC9} + 8.742$	$R^2_{\text{int}} = 0.850$ $R^2_{\text{adj}} = 0.800$ $Q^2_{\text{cv}} = 0.745$	$R^2_{\text{ext}} = 0.877$
3 $Y = -1.793 \times 10^{-5} \cdot \text{ATS7m} - 0.310 \cdot \text{AATS1s}$ $- 2.023 \cdot \text{GATS4c} + 0.080 \cdot \text{VR3\_Dzp}$ $+ 0.058 \cdot \text{VR3\_Dzs} + 5.578$	$R^2_{\text{int}} = 0.844$ $R^2_{\text{adj}} = 0.792$ $Q^2_{\text{cv}} = 0.723$	$R^2_{\text{ext}} = 0.833$
4 $Y = -9.457 \times 10^{-5} \cdot \text{ATS1m} - 0.323 \cdot \text{AATS1s}$ $- 2.032 \cdot \text{GATS4c} + 0.081 \cdot \text{VR3\_Dzp}$ $+ 0.062 \cdot \text{VR3\_Dzs} + 5.877$	$R^2_{\text{int}} = 0.838$ $R^2_{\text{adj}} = 0.784$ $Q^2_{\text{cv}} = 0.722$	$R^2_{\text{ext}} = 0.814$

**Figure 2:** Plot of residuals and experimental activities for the internal and external datasets.

Compound 1 interacted with specific active residues of  $\alpha$ -amylase. These interactions involved the formation of a hydrogen bond with His305, as well as carbon–hydrogen bonds with His201, Asp300, and Glu233. In addition, a pi–pi-T-shaped interaction occurred between compound 1 and His201, where the electron clouds of aromatic rings overlapped. Furthermore, compound 1 exhibited pi–alkyl interactions with Trp59, Tyr62, His299, Leu162, and Ala198. These interactions collectively contributed to a MolDock score of  $-154.05$ , which represents the binding potential of compound 1. Figure 6 provides a visual representation of

compound 1's arrangement within  $\alpha$ -amylase, in both 2D and 3D formats.

Compound 2 interacted with specific residues in the active site of  $\alpha$ -amylase. These interactions included hydrogen bonds with Thr163, Tyr62, His101, and Asp300, as well as carbon–hydrogen bonds with His299 and Asp300. Additionally, a pi–sigma interaction occurred with Trp59 and His305, and a pi–pi stacking interaction occurred among Tyr62, Trp58, and Trp59. Furthermore, pi–alkyl interactions were observed with Trp59. Collectively, these interactions contributed to a score of  $-150.18$ , indicating the

**Table 3: Definitions, class, VIF,  $M_x$ , and P-values of the descriptors selected for Equation (1).**

Descriptor	Definition	Class	VIF	$M_x$	P-value
ATS4i	Broto–Moreau autocorrelation, lag 4, weighted by first ionization potential	2D	6.18	−0.30	3.73E-03
GATS4c	Geary autocorrelation, lag 4, weighted by charges	2D	3.40	0.50	5.18E-08
VR3_Dzp	Logarithmic Randic-like eigenvector-based index from Barysz matrix, weighted by polarizabilities	2D	2.70	−0.36	1.52E-08
VR3_Dzs	Logarithmic Randic-like eigenvector-based index from Barysz matrix, weighted by I-state	2D	2.29	−0.29	2.26E-08
piPC9	Conventional bond order ID number of order $9(\ln(1 + x))$	2D	8.58	1.45	5.90E-04

**Table 4: Y-permutation studies.**

Model	R	R <sup>2</sup>	Q <sup>2</sup>
Original	0.888	0.789	0.662
Random 1	0.289	0.084	-0.335
Random 2	0.354	0.126	-0.523
Random 3	0.305	0.093	-0.350
Random 4	0.319	0.102	-0.253
Random 5	0.386	0.149	-0.366
Random 6	0.263	0.069	-0.478
Random 7	0.375	0.140	-0.495
Random 8	0.416	0.173	-0.339
Random 9	0.614	0.377	-0.262
Random 100.672	0.452	0.167	

Random model parameters  
Average R = 0.399  
Average R<sup>2</sup> = 0.176  
Average Q<sup>2</sup> = -0.323  
cRp<sup>2</sup> = 0.705

binding affinity of compound 2. Figure 7 provides a visual representation of compound 2 within the active site of  $\alpha$ -amylase, depicted in both 2D and 3D diagrams.

Compound 3, which had the highest MolDock score, -154.33, demonstrated strong interactions within the active site of  $\alpha$ -amylase. These interactions included conventional hydrogen bonds with Thr163, His305, Glu233, Asp300, Asp197, and His299. Additionally, a pi-sigma interaction with Trp59 and a pi-pi stacking interaction with Tyr62 were observed. Notably, alkyl interactions were observed with Ala106 and Val107, and a pi-alkyl interaction occurred with Leu165. These interactions collectively contributed to the high MolDock score of compound 3, which indicated its favorable binding affinity. Figure 8 depicts the interactions of compound 3 within the active site of  $\alpha$ -amylase, in both 2D and 3D representations.

Compound 4, with a score of -150.06, exhibited interactions within the active site of the enzyme. These interactions involved a carbon-hydrogen bond with Tyr151 and His201, as well as a pi-donor hydrogen bond with Trp59. Additionally, alkyl interactions were observed with Leu165, and pi-alkyl interactions occurred with Tyr62, His305, and Leu162. These interactions collectively contributed to the overall score of compound 4, thus suggesting its binding potential. Figure 9 depicts the interactions of compound 4 within the active site of the enzyme, in both 2D and 3D representations.

Compound 5 interacted with  $\alpha$ -amylase through conventional hydrogen bonds with Thr163, and carbon-hydrogen bonds with His101, Glu233, Asp300, Asp197, and His299. Additionally, a pi-pi stacking interaction with Tyr62 and pi-alkyl interactions with Trp59 and Leu165 were observed. These interactions collectively contributed to a MolDock score of -151.14, which indicated the binding strength of compound 5. Figure 10 depicts the interactions of compound 5 in the active site of the  $\alpha$ -amylase enzyme, in both 2D and 3D.

#### *Drug similarity and pharmacokinetic properties of the designed compounds*

Drug similarity studies were conducted with four sets of rules: the rule of five, Veber rule, Egan rule, and Muegge rule (Table 6). These rules were used to assess the drug-likeness of the compounds and predict their bioavailability. None of the compounds violated more than two of these rules, thus suggesting favorable drug-like properties and likelihood of being orally safe (Table 6).

Furthermore, the pharmacokinetic studies provided insights into the absorption and distribution potential of the compounds (Table 6). The compounds, except for compounds 4 and 5, exhibited high absorption potential

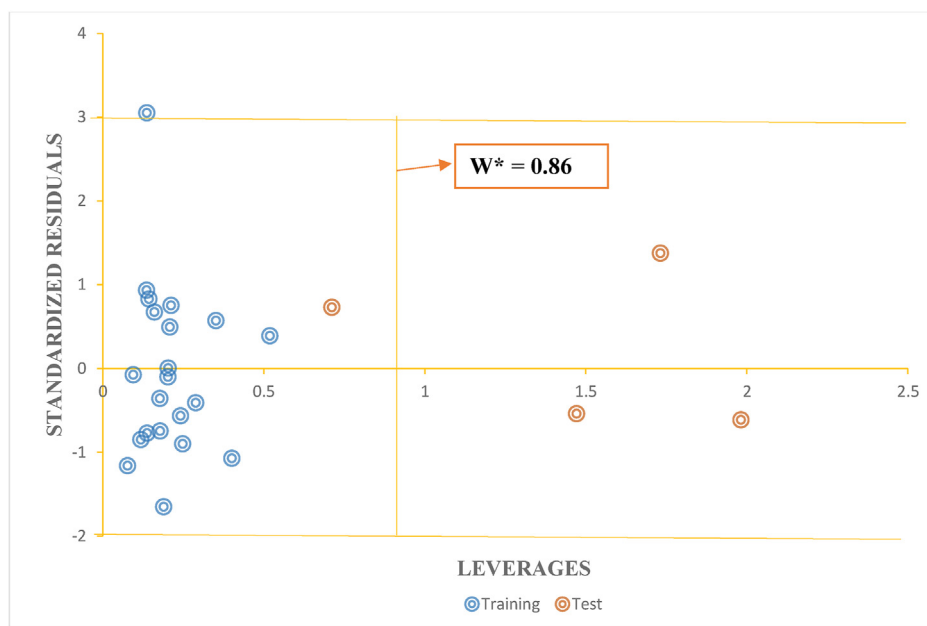


**Figure 3:** Plot of standardized residuals against the leverage values.

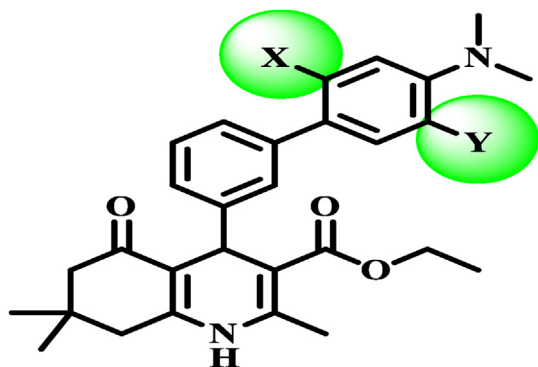


**Figure 4:** Template compound for the design, with a score of  $-149.8$  and predicted activity of  $5.220$ .

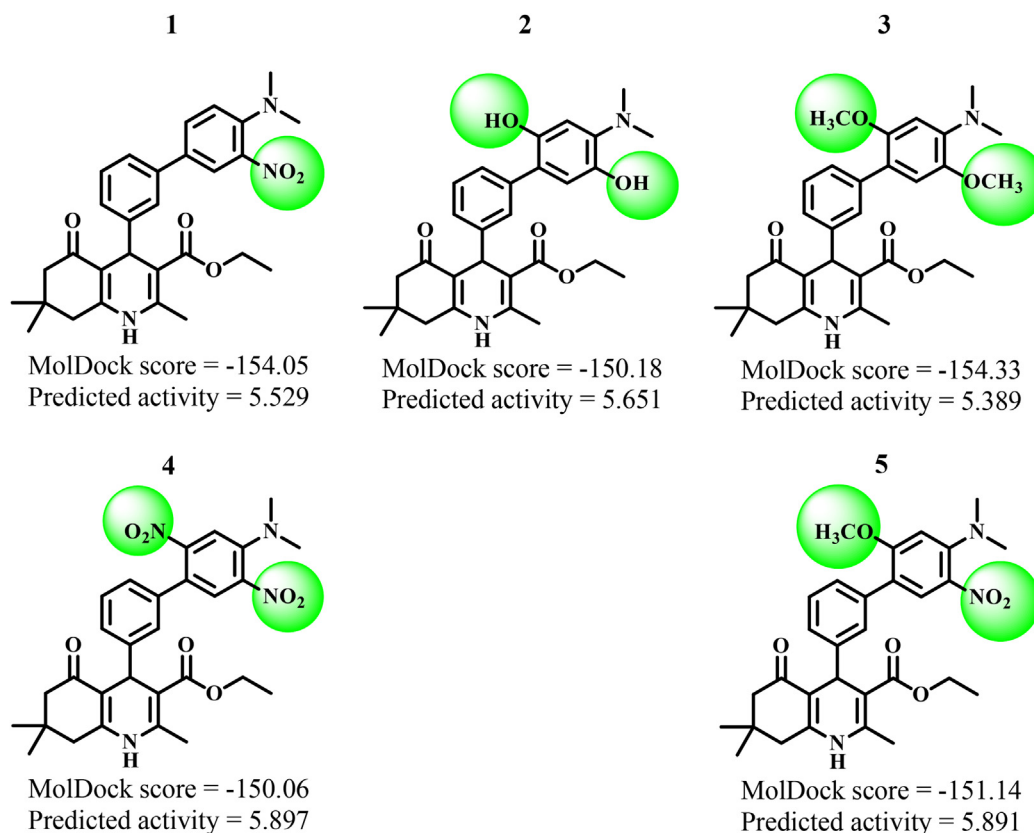
and thus should be effectively absorbed through the gastrointestinal tract. However, the compounds were found to be unable to cross the blood–brain barrier (BBB) and therefore do not appear to have substantial brain penetration properties. Most compounds (except compound 4) were identified as substrates of P-glycoprotein (P-gp), a transporter protein involved in the efflux of drugs. Being a P-gp substrate affects the distribution and elimination of a compound. Moreover, the compounds were found to be inhibitors of several CYP enzymes, namely 2C19, 2C9, and 3A4. CYP enzymes play crucial roles in drug metabolism (Table 6).

Figure 11 presents the bioavailability of the designed compounds. The colored region in the figure indicates the range of physicochemical properties considered appropriate for achieving oral bioavailability. Notably, all designed compounds except compound 4 were within this region, thus indicating that they have the necessary characteristics to be effectively absorbed when taken orally; i.e., they are likely to be orally bioavailable.

## Discussion

The antidiabetic medications currently available on the market often have substantial adverse effects, thus limiting their use and posing challenges for patients.<sup>2</sup> Therefore, alternative drugs must be developed that not only improve therapeutic outcomes, but also are more convenient and accessible for patients. Yousuf et al. have highlighted the need for further exploration of 1,4-DHP derivatives through *in silico* investigations, with the ultimate goal of discovering new antidiabetic drugs that inhibit  $\alpha$ -amylase.

Of the four equations created with GFA, which allows for multiple equations to be generated and provides flexibility in selection,<sup>12</sup> Equation (1) was optimal. This equation was chosen because of its favorable characteristics, including its high internal and external assessment scores, its ability to explain a substantial portion of the variation in biological activity, its reliable performance estimation, its strong performance when applied to external test set data, and its excellent predictive ability for the derivatives under study.



**Figure 5:** The designed compounds, with MolDock scores and predicted activity.

Table 5: Scores and various interactions of the designed compounds and the standard drug.

S/ N	MolDock scores	Conventional hydrogen bond	Carbon-hydrogen bond	$\pi$ - $\pi$ T-shaped	$\pi$ -donor hydrogen bond	$\Pi$ -sigma	$\pi$ - $\pi$ stacked	Alkyl	$\pi$ -alkyl
1	-154.05	His305.	His201, Asp300, Glu233.	His201.	-	-	-	-	Trp59, Tyr62, His299, Leu162, Ala198.
2	-150.18	Thr163, Tyr62, His101, Asp300.	His299, Asp300.	-	-	Trp59, His305.	Tyr62.	-	Trp58, Trp59.
3	-154.33	Thr163.	His305, Glu233, Asp300, Asp197, His299.	-	-	Trp59.	Tyr62.	Ala106, Val107.	Leu165.
4	-150.06	-	Tyr151, His201.	-	Trp59.	-	-	Leu165.	Tyr62, His305, Leu162.
5	-151.14	Thr163.	His101, Glu233, Asp300, Asp197, His299.	-	-	-	Tyr62.	-	Trp59, Leu165.

Therefore, it was considered the most suitable equation among the alternatives, yielding the most credible predictions of the activities of the newly designed compounds.

Additionally, a comprehensive statistical analysis was performed on the chosen equation. The VIF, mean effect values, P-values, and Y-permutation test were performed on the selected equation. The statistical analysis strongly suggested that the selected equation was valid, reliable, and capable of accurately predicting the activities of the derivatives. The absence of multicollinearity among the descriptors, the significant effects of the descriptors on the equation, the statistical significance of the descriptors, and the non-random nature of the equation's relationship with activity all contributed to the overall confidence in the equation's performance and its utility in predicting the activities of the derivatives under investigation.

A plot of standardized residual values against leverages was subsequently generated to examine the effects of individual compounds on the performance of the equation.<sup>16</sup> This plot helps identify compounds that significantly influence the equation, because of their leverage values or their standardized residuals.<sup>16</sup> Compounds 23, 25, and 26 influenced the equation's performance. These compounds exhibited leverage values above the threshold value. Compound 9 was identified as an outlier: it may have structural incompatibility with the target's binding site, lacking the necessary features to effectively interact with the target, thus causing it to deviate from the expected behavior. Therefore, this compound cannot be considered a template for designing new drugs.

Compound 19 was chosen as a template for the design of new compounds. The selection of this compound was based on its high MolDock score, indicating its favorable binding affinity to the target active site. In designing new compounds, we made modifications by adding  $-\text{OCH}_3$  and  $-\text{NO}_2$  groups at the X and Y positions on the template. This addition of these groups enhanced the binding affinity of the newly designed compounds. The observed improved binding affinity was attributed to the stability achieved through resonance. The presence of the  $-\text{OCH}_3$  and  $-\text{NO}_2$  groups in the specific positions created a resonance effect, thereby enhancing the overall stability of the molecule and facilitating stronger interactions at the target's active site. Additionally, the newly designed compounds exhibited enhanced predictive capability surpassing that of the template compound. The results of these studies indicated that the designed compounds exhibited stronger binding affinity, as evidenced by higher MolDock scores, than the template compound and acarbose.

Moreover, the designed compounds exhibited favorable drug profile characteristics. Their adherence to multiple drug-likeness rules suggested their potential to be safe and suitable for oral administration. These rules serve as guidelines to assess the likelihood of a compound's being a successful drug candidate.

Furthermore, the designed compounds had high absorption potential, thus suggesting that they can be efficiently absorbed into the bloodstream after oral administration. This factor is important, because it determines the bioavailability and effectiveness of a drug.

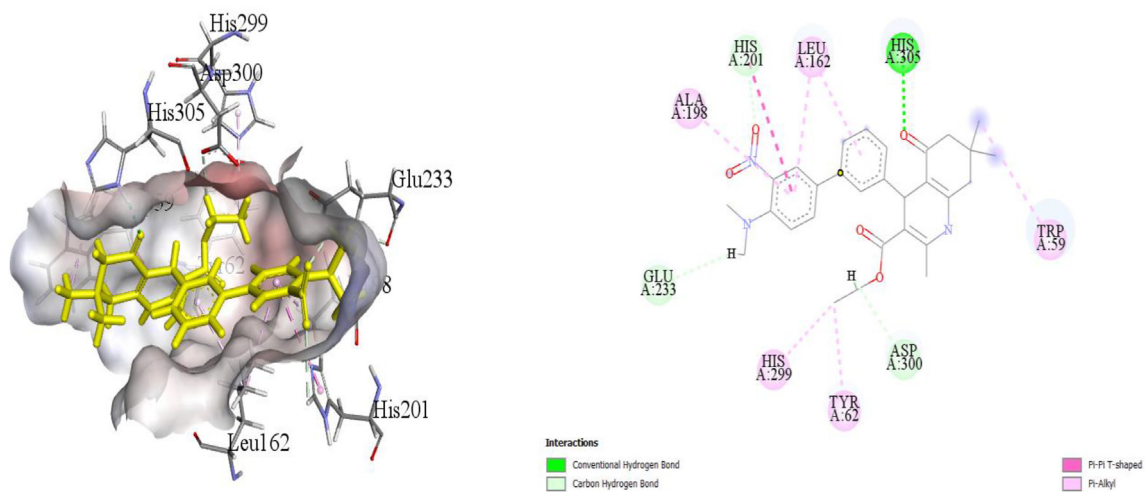


**Figure 6:** The 2D and 3D diagrams of compound 1 within the active site of  $\alpha$ -amylase.

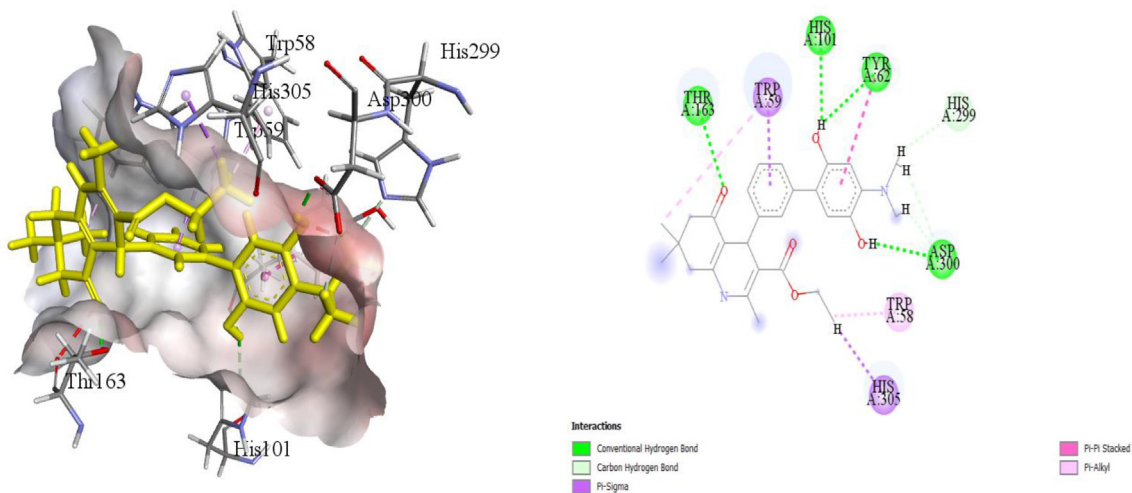


**Figure 7:** The 2D and 3D diagrams of compound 2 within the active site of  $\alpha$ -amylase.

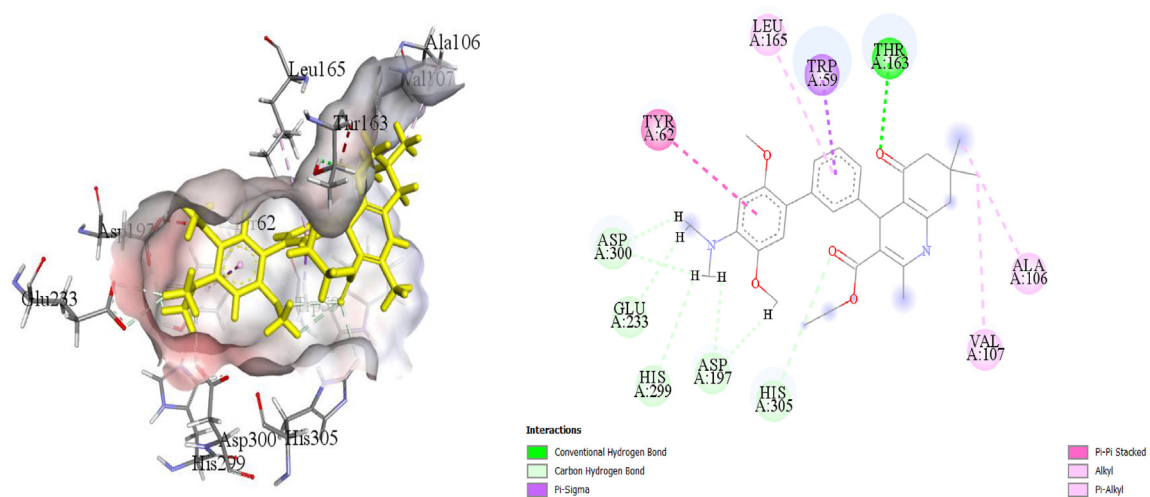


**Figure 8:** The 2D and 3D diagrams of compound 3 within the active site of  $\alpha$ -amylase.

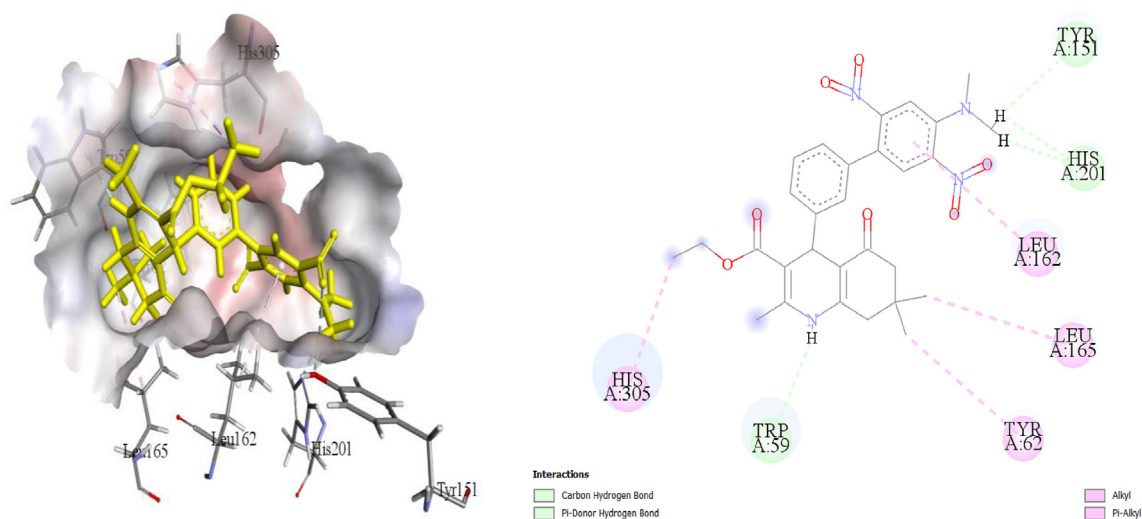


**Figure 9:** The 2D and 3D diagrams of compound 4 within the active site of  $\alpha$ -amylase.

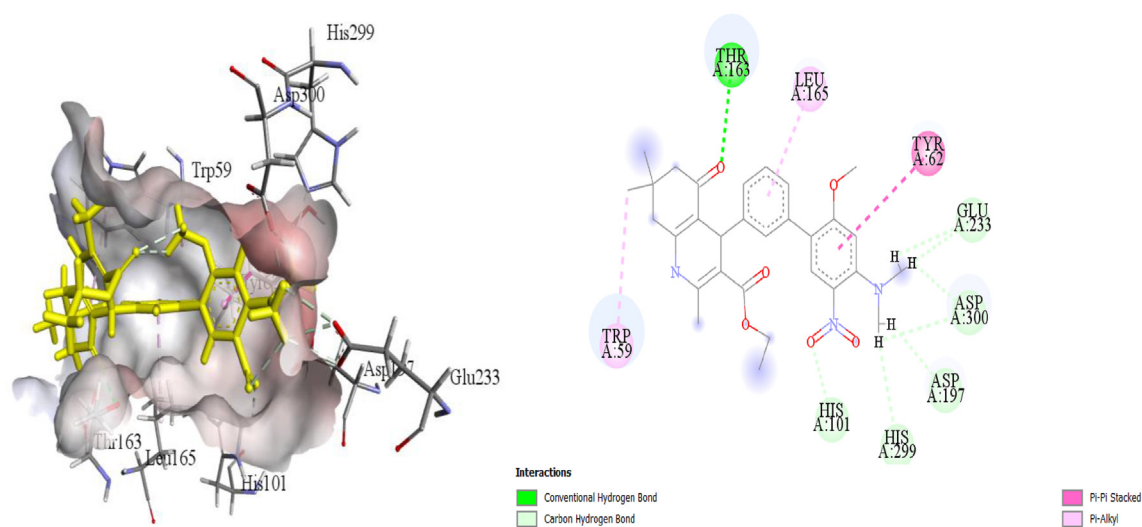


**Figure 10:** The 2D and 3D diagrams of compound 5 within the active site of  $\alpha$ -amylase.

Additionally, the compounds demonstrated limited brain permeability, and consequently low likelihood of penetrating the BBB, thereby decreasing their likelihood of affecting the central nervous system. This aspect may advantageously decrease potential adverse effects associated with the central nervous system.

Moreover, the finding that the compounds are P-gp substrates further supports their potential as viable drug candidates. P-gp is a protein that transports substances including drugs in cells.<sup>23</sup> Compounds that are P-gp substrates are likely to be effectively transported and distributed within the body, thus improving their overall efficacy.

**Table 6: The drug-like and pharmacokinetic studies of the designed compounds.**

S/ N	Drug-likeness properties					Pharmacokinetic properties							
	Rule of 5	Veber rule	Egan rule	Muegge rule	Bioavailability score	GI absorption	BBB permeation	P-gp substrate	CYP Inhibitors				
									1A2	2C19	2C9	2D6	3A4
1	1	0	0	1	0.55	High	No	Yes	No	Yes	Yes	No	Yes
2	0	0	0	0	0.55	High	No	Yes	No	Yes	Yes	No	Yes
3	1	0	0	1	0.55	High	No	Yes	No	Yes	Yes	Yes	Yes
4	2	1	1	2	0.17	Low	No	No	No	No	Yes	No	Yes
5	1	0	0	1	0.55	Low	No	Yes	No	Yes	Yes	No	Yes



**Figure 11:** Bioavailability of the designed compounds.

## Conclusions

Our results indicated that Equation (1), derived from the GFA, had the highest accuracy, on the basis of both internal and external assessment parameters, including  $R^2_{\text{int}} = 0.852$ ,  $R^2_{\text{adj}} = 0.803$ ,  $Q^2_{\text{cv}} = 0.731$ , and  $R^2_{\text{ext}} = 0.884$ . Moreover, compound 19 was chosen as a template because of its favorable MolDock score of  $-149.8$ . By introducing structural modifications, we created five potent analogs based on this template. Notably, these designed compounds demonstrated favorable interactions within the active site of  $\alpha$ -amylase, with scores surpassing those of both the template compound and acarbose. Additionally, comprehensive studies on the drug-like properties and pharmacokinetics supported the designed compounds' oral safety and favorable pharmacokinetics profiles. Consequently, our findings suggest that the designed compounds have potential for further exploration in the quest for new anti-diabetic agents.

## Source of funding

This research did not receive any specific grant from funding agencies in the public, commercial, or not-for-profit sectors.

## Conflict of interest

The authors have no conflict of interest to declare.

## Ethical approval

There are no ethical issues.

## Consent

Not applicable.

## Authors contributions

The research idea was conceived by AU and KSA. KSA conducted all computational analysis and wrote the manuscript. AU, KSA, SEA, GAS, and ABU collectively reviewed the results to ensure minimal errors. AU supervised the project and carefully proofread the manuscript. All authors have critically reviewed and approved the final draft and are responsible for the content and similarity index of the manuscript.

## Acknowledgment

We acknowledge Ahmadu Bello University for providing the softwares used in the study.

## Availability of data and materials

All data produced or examined during this study are included in this published article.

## References

- Hermansen K, Mortensen LS, Hermansen ML. Combining insulins with oral antidiabetic agents: effect on hyperglycemic control, markers of cardiovascular risk and disease. **Vasc Health Risk Manag** 2008; 4(3): 561–574. <https://doi.org/10.2147/vhrm.s1815>.
- Aminu KS, Uzairu A, Umar AB, Ibrahim MT. Salicylic acid derivatives as potential  $\alpha$ -glucosidase inhibitors: drug design, molecular docking and pharmacokinetic studies. **Bull Natl Res Cent** 2022; 46: 162. <https://doi.org/10.1186/s42269-022-00853-6>.
- Sunusi K, Uzairu A, Eyije S, Adamu G, Bello A. Ligand-based drug design, molecular docking and pharmacokinetic studies of some series of 1,4 – dihydropyridines derivatives as human intestinal maltase-glucoamylase inhibitor. **Chem Data Collect** 2022; 41(April): 100911. <https://doi.org/10.1016/j.cdc.2022.100911>.
- Birt DF, Boylston T, Hendrich S, Jane JL, Hollis J, Li L, et al. Resistant starch: promise for improving human health. **Adv Nutr** 2013; 4(6): 587–601. <https://doi.org/10.3945/an.113.004325>.
- Nichols BL, Quezada-Calvillo R, Robayo-Torres CC, Ao Z, Hamaker BR, Butte NF, et al. Mucosal maltase-glucoamylase plays a crucial role in starch digestion and prandial glucose homeostasis of mice. **J Nutr** 2009; 139(4): 684–690. <https://doi.org/10.3945/jn.108.098434>.
- Pérez-Ros P, Navarro-Flores E, Julián-Rochina I, Martínez-Arnau FM, Cauli O. Changes in salivary amylase and glucose in diabetes: a scoping review. **Diagnostics** 2021; 11(3): 453. <https://doi.org/10.3390/diagnostics11030453>.
- de Souza PM, de Oliveira Magalhães P. Application of microbial  $\alpha$ -amylase in industry – a review. **Braz J Microbiol** 2010; 41(4): 850–861. <https://doi.org/10.1590/S1517-83822010000400004>.
- Gong L, Feng D, Wang T, Ren Y, Liu Y, Wang J. Inhibitors of  $\alpha$ -amylase and  $\alpha$ -glucosidase: potential linkage for whole cereal foods on prevention of hyperglycemia. **Food Sci Nutr** 2020; 8(12): 6320–6337. <https://doi.org/10.1002/fsn3.1987>.
- Ling Y, Hao ZY, Liang D, Zhang CL, Liu YF, Wang Y. The expanding role of pyridine and dihydropyridine scaffolds in drug design. **Drug Des Dev Ther** 2021; 15: 4289–4338. <https://doi.org/10.2147/DDDT.S329547>.
- Lawal HA, Uzairu A, Uba S. QSAR, molecular docking, design, and pharmacokinetic analysis of 2-(4-fluorophenyl)imidazol-5-ones as anti-breast cancer drug compounds against MCF-7 cell line. **J Bioenerg Biomembr** 2020; 52(6): 475–494. <https://doi.org/10.1007/s10863-020-09858-0>.
- Aminu KS, Uzairu A, Umar AB, Abechi SE, Adamu G. A search for novel antidiabetic agents using ligand-based drug design and molecular docking studies employing human intestinal maltase-glucoamylase as model enzyme. **Adv J Chem A** 2023; 6(2): 155–171. [10.22034/AJCA.2023.387041.1355](https://doi.org/10.22034/AJCA.2023.387041.1355).
- Abdullahi SH, Uzairu A, Ibrahim MT, Umar AB. Chemoinformatics activity prediction, ligand based drug design, Molecular docking and pharmacokinetics studies of some series of 4, 6-diaryl-2-pyrimidinamine derivatives as anti-cancer agents. **Bull Natl Res Cent** 2021; 45(1). <https://doi.org/10.1186/s42269-021-00631-w>.
- Ugbe FA, Shallangwa GA, Uzairu A, Abdulkadir I. Activity modeling, molecular docking and pharmacokinetic studies of some boron-pleuromutilins as anti-wolbachia agents with potential for treatment of filarial diseases. **Chem Data Collect** 2021; 36(September):100783. <https://doi.org/10.1016/j.cdc.2021.100783>.
- Taylor P, Kennard RW, Stone LA. Technometrics computer aided design of experiments. **Technometrics** 2012; 37–41. February 2014.
- Ebuka D, Soliman MES, Elijah S, Adedirin O, Peter F. Qsar and molecular docking study of gonadotropin-releasing hormone receptor inhibitors. **Sci Afr** 2022; 17:e01291. <https://doi.org/10.1016/j.sciaf.2022.e01291>.
- Ibrahim MM, Uzairu A, Ibrahim MT, Umar AB. Modelling PIP4K2A inhibitory activity of 1,7-naphthylidene analogues using machine learning and molecular docking studies. **RSC Adv** 2023; 13(6): 3402–3415. <https://doi.org/10.1039/d2ra07382j>.
- Aouidate A, Ghaleb A, Ghamali M, Chtita S, Ousaa A, Choukrad M, et al. QSAR study and rustic ligand – based virtual screening in a search for aminooxadiazole derivatives as PIM1 inhibitors. **Chem Cent J** 2018; 1–12. <https://doi.org/10.1186/s13065-018-0401-x>.
- Kar S, Chatterjee S. In silico meets in vitro techniques in ADMET profiling of drug discovery (Part I). **Curr Drug Metab** 2020; 21(10). <https://doi.org/10.2174/138920022110201126153901>, 745–745.
- Batool M, Ahmad B, Choi S. A structure-based drug discovery paradigm. **Int J Mol Sci** 2019; 20(11): 2783. <https://doi.org/10.3390/ijms20112783>.
- Glassman PM, Muzykantov VR. Pharmacokinetic and pharmacodynamic properties of drug delivery systems. **J Pharmacol Exp Ther** 2019; 370(3): 570–580. <https://doi.org/10.1124/jpet.119.257113>.
- Palleria C, Di Paolo A, Giofrè C, Caglioti C, Leuzzi G, Siniscalchi A, et al. Pharmacokinetic drug-drug interaction and their implication in clinical management. **J Res Med Sci** 2013; 18(7): 601–610.
- Yousuf H, Shamim S, Mohammed K, Chigurupati S. Bio-organic chemistry dihydropyridines as potential  $\alpha$ -amylase and  $\alpha$ -glucosidase inhibitors: synthesis, in vitro and in silico studies. **Bioorg Chem** 2020; 96(August 2019): 103581. <https://doi.org/10.1016/j.bioorg.2020.103581>.
- Ahmed Juvale II, Abdul Hamid AA, Abd Halim KB, Che Has AT. P-glycoprotein: new insights into structure, physiological function, regulation and alterations in disease. **Heliyon** 2022; 8(6): e09777. <https://doi.org/10.1016/j.heliyon.2022.e09777>.

**How to cite this article:** Aminu KS, Uzairu A, Abechi SE, Shallangwa GA, Umar AB. Activity prediction, structure-based drug design, molecular docking, and pharmacokinetic studies of 1,4-dihydropyridines derivatives as  $\alpha$ -amylase inhibitors. *J Taibah Univ Med Sc* 2024;19(2):270–286.